Available online at www.sciencedirect.com
SCIENCE DIRECT
Journal of Molecular Catalysis A: Chemical 243 (2006) 1–7
JOURNAL OF MOLECULAR CATALYSIS A: CHEMICAL
www.elsevier.com/locate/molcata

H-MOR: Density functional investigation for the relative strength of Brønsted acid sites and dynamics simulation of NH_3 protonation–deprotonation

M. Elanany [a,1], D.P. Vercauteren [a], M. Koyama [b], M. Kubo [b], P. Selvam [c], E. Broclawik [b], A. Miyamoto [b,d,*]

[a] *Department of Chemistry, University of Namur, Rue de Bruxelles 61, Namur B-5000, Belgium*
[b] *Department of Applied Chemistry, Graduate School of Engineering, Tohoku University, 6-6-11-1302 Aoba, Aramaki, Aoba-ku, Sendai 980-8579, Japan*
[c] *Department of Chemistry, Indian Institute of Technology Bombay, Powai, Mumbai 400 076, India*
[d] *New Industry Creation Hatchery Centre, Tohoku University, 6-6-10 Aoba, Aramaki, Aoba-ku, Sendai 980-8579, Japan*

Received 20 June 2005; received in revised form 2 August 2005; accepted 2 August 2005
Available online 5 October 2005

Abstract

The adsorption energies of NH_3 at different positions in acidic mordenite, viz., main channel, side pocket, and double four-membered rings, are investigated using periodic density functional theory method. Furthermore, for the first time, the dynamic behavior of NH_3 interacting with Brønsted acid site in the main channel has been monitored. The results reveal that the adsorption energies of ammonia on Brønsted acid sites in the main channel (T_4, T_2, and T_1) are higher than that in the side pocket (T_3). Consequently, the strength of Brønsted acid sites follows the same order. Ammonia dynamics results show that the protons are in continuous transfer, where NH_3 acts as a bridge for transferring protons in between ammonium ion and framework oxygen ions.

Keywords: Mordenite; Brønsted acid sites; Ammonia adsorption; DFT; Molecular dynamics

1. Introduction

In the field of heterogeneous catalysis by molecular sieves, ammonia is extensively used as a basic probe molecule for acidity characterization owing to its accessibility for all acid sites locating in pores, channels, or windows ≥4 Å. Some of the encountered problems on using NH_3, in experimental studies, are: (i) strong basicity, which levels out the clear distinction of different acid sites, (ii) the inherent complexity of the vibrational spectra of NH_4^+ and coordinated NH_3, and (iii) its dissociation on some oxide surfaces. These observations led to the use of other probes viz., CO, pyridine, alkyl amines, and alkylnitriles [1–4]. However, many valuable quantitative analyses were carried out by fostering the above-mentioned problems on using NH_3 as a probe [5–8]. Recently, we have shown that the adsorption energy of NH_3 can be effectively used to determine the relative strength of Brønsted acid sites, in isomorphously substituted chabazite, and aluminophosphate-34 [9], and Lewis acid sites in microporous molecular sieves [10]. Lamberov et al. [11] showed that NH_3 is more appropriate than CO as a probe for different Lewis acid sites in molecular sieves. Hence, ammonia adsorption is important to scale the strength of different acid sites in microporous molecular sieves. It is well accepted that the interaction between NH_3 and Brønsted acid sites, in zeolites, is strong enough to form NH_4^+ [12]. Earlier studies indicated the possible interaction of ammonia with the lattice oxygen ions around aluminum site via two, three, or four hydrogen bonds [13–15].

* Corresponding author. Tel.: +81 22 217 7233; fax: +81 22 795 7235.
E-mail address: miyamoto@aki.che.tohoku.ac.jp (A. Miyamoto).
[1] On leave from Department of Chemistry, Faculty of Science, Sohag 82524, Egypt.

1381-1169/$ – see front matter © 2005 Elsevier B.V. All rights reserved.
doi:10.1016/j.molcata.2005.08.014

The important zeolite structure, mordenite (MOR), is known by its pronounced acidity among many other zeolite structures [6,7]. This has led to the use of mordenite for several applications e.g., cracking, isomerization of hydrocarbons, dewaxing of heavy petroleum fractions [16,17]. Therefore, detailed characterization of various acid sites in mordenite is a significant issue for manipulating and understanding its catalytic applications. Moreover, investigating the dynamic behavior of an adsorbate interacting with its host framework will enrich our understanding on how adsorption and desorption processes are taking place at a specific acid site. The two most popular types of computer simulations are Monte Carlo (MC) and molecular dynamics (MD) techniques. MD is more expensive than MC. However, MD simulation is usually more revealing because it provides information on how molecules move. Thus, with MD one can study time dependent phenomena, fluid flow, and other transport phenomena, which cannot be done with MC [18]. Dynamics of several adsorbates as, H_2O [19,20] and CH_3OH [21,22] in zeolites have been studied. Furthermore, the spontaneous proton transfer in between framework oxygen ions of mordenite has been observed recently [23]. Temperature-programmed desorption (TPD) and microcalorimetry techniques (MC) are commonly used for acidity characterization. However, the assignment of its responses to specific acid sites is still unclear. Further, the results depend directly on the experimental conditions [24]. To the best of our knowledge measuring the strength order of Brønsted sites in mordenite could not be tackled in the previous experimental or theoritical studies [4,15, and 25]. This may be due to the complexity of the spectra of probe molecules inside zeolite lattices. Therefore, the aim of this study is to find out the relative strength of Brønsted acid sites in mordenite using NH_3 as a basic probe and to monitor the interaction of NH_3 with Brønsted acid site in the main channel using a novel quantum chemical molecular dynamics (QCMD) code [26].

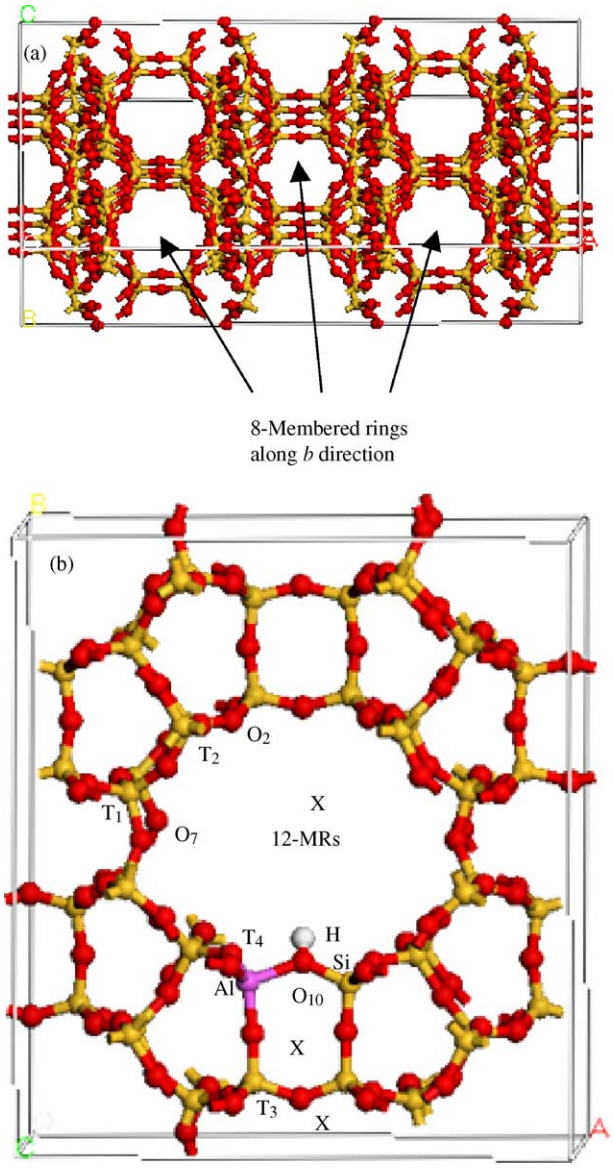

Fig. 1. The optimized structure of acidic mordenite (H-MOR) showing the eight-membered rings along *b* direction (a), and the investigated adsorption sites marked by *x* (b).

2. Theory

2.1. Models

Mordnite has an orthorhombic unit cell. In order to create a Brønsted acid site, in silicalite structure, one silicon is replaced by aluminum and proton (H Al Si47 O96). The proton is attached to the bridging oxygen by covalent bond. The main channel (6.7 Å × 7.0 Å) in [0 0 1] direction consists of 12-membered ring (MR) connected with 8-MR side pocket in the [0 1 0] direction as shown in Fig. 1a and b [27]. For labeling the atoms, we followed Alberti et al. notation [28]. It should be mentioned that there are four distinct tetrahedral (T) sites per unit cell: three lies in the main channel T_4, T_2, T_1 and one in the side pocket T_3 (Fig. 1b). Replacement of Si by (Al, H) has been done to produce Brønsted sites. The protons were attached to O_{10}, O_2, O_7, which are accessible to the interaction with adsorbates in main channel and O_9 in side pocket. There are 14 possibilities for placing the proton in the unit cell. Brändle and Sauer [29] and Demuth et al. [30] have found that T_4 is the most preferable location for sitting Al. Hence, we have chosen this site for investigating the dynamics of NH_3 where the proton (H_1) is attached to O_{10}. Here we are interested in high Si/Al ratio, which permits studying the isolated Brønsted acid sites in MOR and could be extended to mesostructures or amorphous materials.

2.2. Computational details

The initial structures of NH_3, H-MOR, and NH_3–H-MOR were optimized by density functional (DF) method at constant pressure employing Dmol^3 program package [31–33],

with Vosko–Wilk–Nusair [34] local density approximation (LDA) and the energies were evaluated at the generalized gradient approximation (GGA) level with Perdew–Wang (PW91) exchange and correlation functionals [35]. Thus, our choice allows for reasonable timing and sufficient accuracy especially when a comparative analysis is the target. Double numerical with polarization (DNP) basis set was used taking into account all core electrons. This basis set is comparable to 6-31G** set, however, the numerical basis set is much more accurate than Gaussian basis set of the same size [31]. The real space cut-off value was set to 5.5 Å, while the convergence criteria were set as follows: energy = 2×10^{-4} Ha; force = 4×10^{-3} Ha/Å; displacement = 0.05 Å. The adsorption energy E_{ads} was calculated as per the following relation.

$$E_{ads} = E_{NH_4\text{-MOR}} - E_{H\text{-MOR}} - E_{NH_3}$$

where $E_{NH_4\text{-MOR}}$, $E_{H\text{-MOR}}$ and E_{NH_3} refer to the total energies for each term. The thermal energy correction to the total energy was not considered here since the frequency calculation for such a large system is still a big computational challenge. Molecular dynamics simulation for NH_3 adsorption on Brønsted acid in the main channel of H-MOR was carried out using "Colors" code, based on the tight binding approximation, for 2000 steps with time intervals of 0.1 fs at ambient temperature and pressure. Parameterization for "Colors" was carried out on the basis of DFT calculations of valence state ionization potential, Slater exponents for the atomic orbitals, and the best fitting of the diatomic potential energy curves in the system. Further details about the code and its parameterization have been given in earlier papers [26,36–38]. Bond population between two atoms X and Y is given by the relation $M_{XY} = \sum_r^{\text{on } X} \sum_s^{\text{on } Y} N_{rs}$, where N_{rs} is the atomic orbital bond population.

3. Results and discussion

3.1. Adsorption of NH_3 in the main channel, side-pocket, and D_4-MRs of H-MOR

Table 1 summarizes the optimized geometrical parameters for H-MOR and NH_4-MOR structures as shown in Fig. 1b and Fig. 2, respectively, as well as the corresponding experimental geometries for natural mordenite with the formula $Na_{1.5}K_{2.8}Ca_{2.1}Al_9Si_{39}O_{96}$ [28]. First, it can be seen from this table that there is a considerable local distortion in the framework upon the substitution $Si^{4+} \rightarrow Al^{3+} + H^+$. This is reflected from the increase of Al–O_{10} bond length (1.897 Å) and the decrease of Al–O_{10}–Si bond angle (138.1°) with respect to T_4–O_{10} (1.637 Å) and T_4–O_{10}–T_4 (146.8°) in natural MOR [28]. In H-MOR, the other Al–O bond lengths viz., Al–O_2 (1.712 Å), Al–O_2' (1.711 Å) and Al–O4 (1.696 Å) are affected slightly by this substitution. After NH_3 adsorption, the Al–O_{10} (1.771 Å) and Al–O_{10}–Si (138.7°) are changed to a small degree with respect to H-MOR due to the formation of NH_4^+ ion. Thus, the local distortion, in the case of H-MOR, is larger than that of NH_4-MOR or natural MOR. A similar observation has been noticed when the optimized geometries of pure silica mordenite, Na-MOR, and H-MOR structures

Table 1
Structural parameters, total energies (au), and Hirshfeld charges for H-MOR and NH_4-MOR at T_4 site

Structural parameters and charges	H-MOR	Experimental [28]	H-MOR [30]		NH_4-MOR
			LDA	GGA	
Si–O_{10}	1.686		1.669	1.682	1.603
Al–O_{10}	1.897	1.637	1.850	1.874	1.771
Al–O_2	1.712	1.614	1.700	1.716	1.771
Al–O_2'	1.711	1.614	1.700	1.716	1.739
Al–O_4	1.696	1.620	1.685	1.700	1.701
O_{10}–H_1	0.982	-	0.995	0.993	1.638
O_2–H_2					1.674
O_2'–H_3					2.618
N–H_1, N–H_2					1.077, 1.037
N–H_3, N–H_4					1.030, 1.027
∠Al–O_{10}–Si	133.2	146.8	136.2	133.3	138.7
∠O_4–Al–O_{10}	104.2	112.4	107.5	107.7	114.8
∠O_2–Al–O_{10}	98.9	105.5	98.5	95.6	101.2
∠O_2'–Al–O_{10}	102.7	105.5	98.5	95.6	103.9
∠O_2–A1–O_{21}	114.7	109.7	113.1	116.6	105.9
∠O_2–A1–O_4	117.8	111.6	117.5	115.8	114.6
qH_1, qH_2	0.220				0.126, 0.123
qH_3, qH_4					0.174, 0.188
qO_{10}, qO_2	−0.163, −0.345				−0.309, −0.343
qO_4, qO_2'	−0.352, −0.352				−0.352, −0.316
qSi, qAl, qN	0.588, 0.516				0.56, 0.495, −0.040
Total energy	−21082.62955				−21139.24742

Interatomic distances are given in (Å) and bond angles in (°).

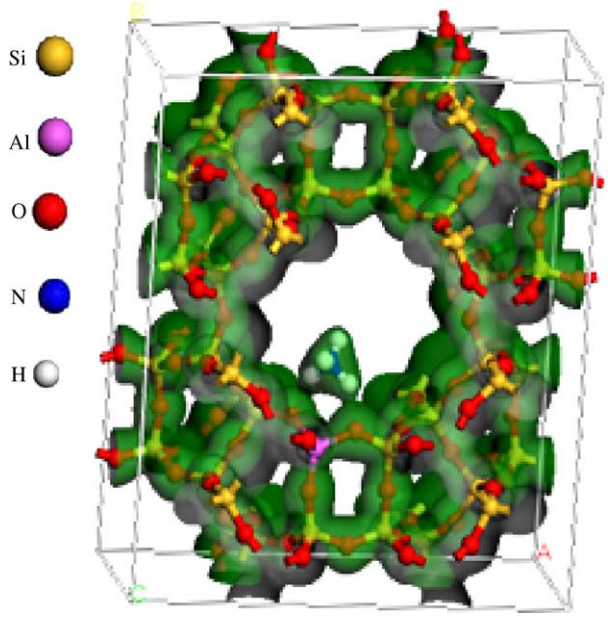

Fig. 2. The optimized structure of NH_4-MOR, the total electron density distribution showing the interaction between NH_4^+ and the lattice oxygen ions.

were compared [30]. The calculated structural parameters by Demuth et al. [30] using DF with plane-wave basis set and LDA or GGA approximations are given in Table 1 for making a comparison with our results. An average difference of ∼0.014 Å in bond lengths and ∼0.8° in bond angles are noticed between our results and Demuth et al. results. This can be attributed to the different bases sets used in the calculations. They showed that the structural parameters obtained by LDA and GGA were in good agreement with the experimental data for natural MOR. However, in the case of H-MOR, the local distortion was larger by using GGA than by using LDA. A recent neutron diffraction study for three deuterated mordenite (D-MOR) samples with Si/Al = 5.5, 5.6, and 10 suggested the presence of four types of Brønsted acid sites at O_{10}, O_9, O_6 and O_5 [39]. However, the relation between the structural parameters and the strength of these sites was unclear. For examples, it was mentioned that the strength of Brønsted acid site decreases with the increase of Al content. Nonetheless, the O_{10}–D bond distances (1.01, 0.99, and 1.00 Å) and T_4–O_{10}–T_4 angles were 136, 156, and 152° for D-MOR with Si/Al = 5.5, 5.6, and 10, respectively. Furthermore, although Al–O is longer than Si–O, the measured T_4–O_{10} bond lengths were 1.63, 1.62, and 1.62 Å for the same samples order. The difficulty to designate the geometrical distortions predicted by computational calculations may be due to the deficiency to determine the exact location of Al or Si in the framework.

The structural parameters during the molecular dynamics simulation are not stable, especially around the adsorption site, due to the thermal energy of the atoms at 298.15 K.

Fig. 2 shows the electron density distribution of NH_3 adsorbed on the Brønsted acid site (T_4–O_{10}H) in the main channel of H-MOR. It is clear that H_1 is transferred to NH_3 molecule to form NH_4-MOR. This is supported by the change of N–H_1 distance (1.077 Å), which becomes comparable to the other N–H bonds in NH_4-MOR, viz., N–H_2 = 1.037 Å, N–H_3 = 1.030 Å, and N–H_4 = 1.027 Å. At the same time, O_{10}–H_1 distance (1.638 Å) is significantly elongated compared to that of H-MOR (see Table 1). Moreover, the negative charge on O_{10} is significantly increased with respect to that in H-MOR. Also, the charge on nitrogen is changed from (−0.3), in free ammonia molecule (E_{NH_3} = −56.56152 a.u.; N–H 1.022 Å), to (−0.04) in NH_4-MOR. All these observations indicate the formation of NH_4^+ ion.

Other adsorption sites viz., main channel (T_2–O_2, T_1–O_7), side pocket (T_3–O_9), and D_4-MRs have been investigated. The calculated geometries and adsorption energies at these sites are summarized in Table 2. In the main channel and D_4-MRs Al occupies T_4, T_2, and T_1 tetrahedral sites while in the side pocket Al occupies T_3 site. Local distortions in the framework and ammonium ion formation on these sites have been observed similarly to the above-discussed T_4 site. The calculated adsorption energies of NH_3 in the main channel at T_4, T_2, and T_1 are −147.9, −142.2, and −146.1 kJ/mol, respectively. These values are in very good agreement with the experimental results obtained by Katada et al. [6,7]. The higher adsorption energy in the main channel than that in the side pocket (−111.0 kJ/mol) indicates that Brønsted acid sites in the main channel are stronger than the Brønsted acid site in the side pocket. This result agrees with an earlier FTIR study using CO and pyridine as probe molecules [1]. In order to see whether the lower adsorption

Table 2
Structural parameters and adsorption energies of NH_3 on H-MOR at main channel, side pocket, and double four-membered rings

Adsorption site	The optimized geometries for H-MOR	Adsorption energy (kJ/mol)
Main channel		
T_4–O_{10}	Si–O, 1.686; Al–O, 1.897; ∠A1–O–Si, 133.2; O–H, 0.982	−147.9
T_2–O_2	Si–O, 1.697; Al–O, 1.895; ∠A1–O–Si, 131.6; O–H, 0.980	−142.2
T_1–O_7	Si–O, 1.676; Al–O, 1.889; ∠A1–O–Si, 131.9; O–H, 1.028	−146.1
Side pocket		
T_3–O_9	Si–O, 1.686; Al–O, 1.898; ∠Al–O–Si, 136.8; O–H, 0.894	−111.0
Double 4-MR	Si–O, 1.573; Al–O, 1.741; ∠Al–O–Si, 159.4	−80.4

Interatomic distances are given in (Å) and bond angles in (°).

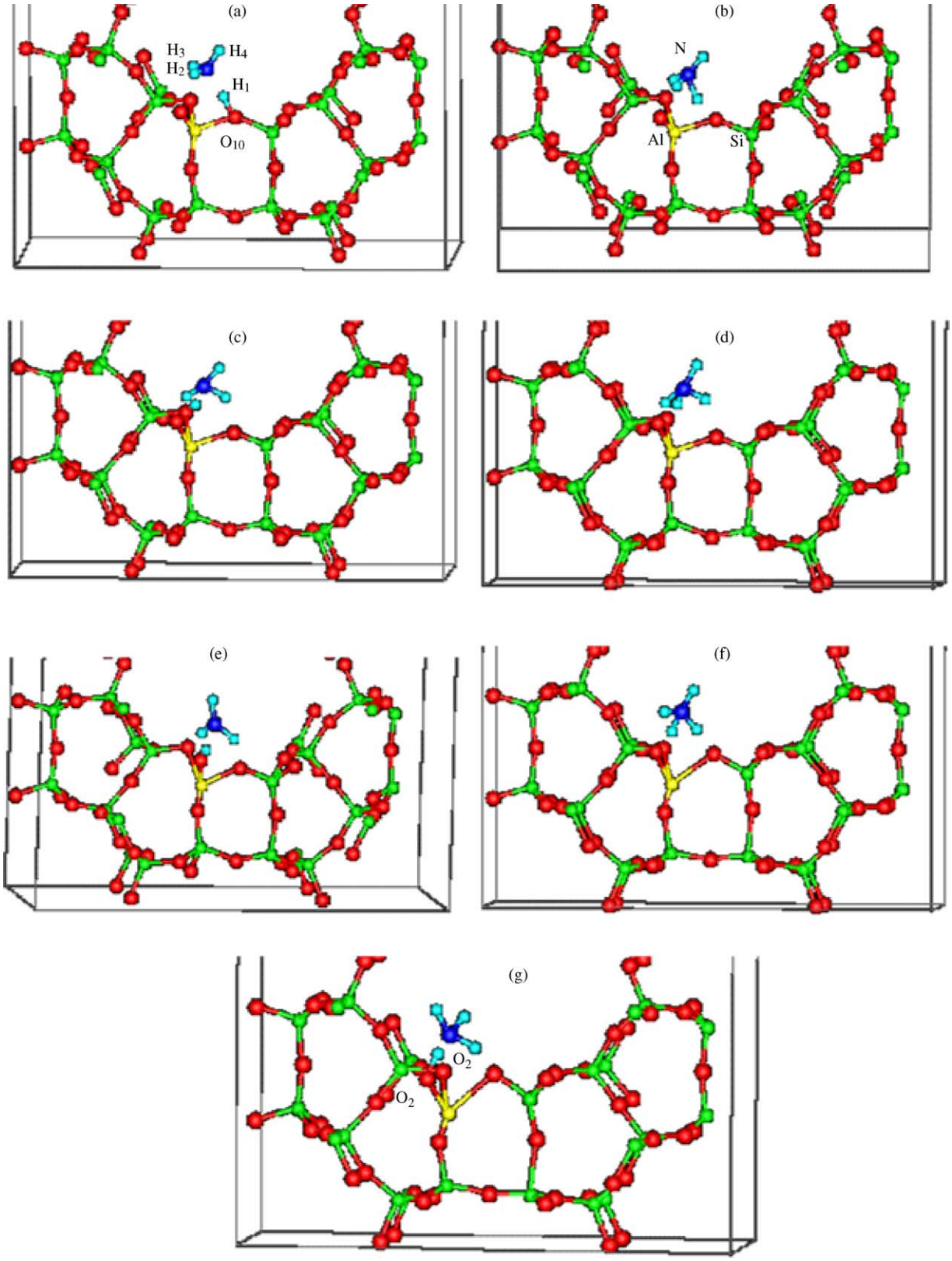

Fig. 3. Snapshots taken during the molecular dynamics simulation of ammonia adsorption on Brønsted acid site in the main channel of H-MOR at various steps at ambient temperature and pressure: (a) 50, (b) 280, (c) 490, (d) 720, (e) 880, (f) 1320 and (g) 2000.

energy of ammonia in the side pocket originates from weak hydrogen bonds to the framework or from the intrinsic acidity, we have calculated the deprotonation energy (DPE) for H-MOR at T_4 and T_3 sites. DPE is defined as the energy required to detach a proton from the framework of H-MOR. The calculated DPE at T_4 (1388.8 kJ/mol) is lower than that at T_3 (1396.5 kJ/mol). Clearly, this indicates that the weaker Brønsted acid site at T_3 is mainly responsible for the lower adsorption energy of ammonia in the side pocket compared to that at T_4 site in the main channel. It should be mentioned here that the calculated DPE value at T_4 site is very close to the calculated value for O'_2H (1388 kJ/mol) by Brändle and Sauer using the hybrid QM-Pot method [29]. The lower adsorption energy in D_4-MR (−80.4 kJ/mol) compared to that in main channel reveals that NH_3 adsorbs preferably in the main channel rather than to be in the D_4-MR. Hence, there are mainly two adsorption sites of NH_3 viz., main channels and side pockets. In the D_4-MR, NH_3 is tricoordinated to the neighboring lattice oxygen ions. Tetra-coordinated ammonium ion has not been observed at the investigated sites in this study.

It is important to note that the calculated adsorption energies of ammonia here are slightly higher than the previously reported values using both bare-cluster models (−114 kJ/mol) [13] and embedded-cluster models (−133 kJ/mol) [29]. This may be due to the enhanced interaction between ammonium ion and the lattice oxygen ion upon using periodic models or to the different functionals used or the two factors together.

Interestingly Demuth et al. [30] have found that the polarity of the chemical bond AlO_{10}–H is influenced by applying GGA, resulting in a stronger AlO_{10}–H bond (see Table 1; O_{10}–H = 0.995 Å by LDA versus 0.993 Å by GGA). Therefore, higher adsorption energy values are expected for structures optimized by LDA. This can explain the relatively higher adsorption energies of ammonia obtained in this study compared to those calculated in previous papers [13,29].

3.2. Dynamics of NH_3 adsorption on the Brønsted acid at T_4 site in main channel of H-MOR

Fig. 3 shows snapshots taken during the molecular dynamics simulation of NH_4^+ interacting with the lattice oxygen ions of MOR structure at different steps. At 50 step the proton H_1 starts to protonate NH_3 molecule. By the 280 step, NH_4^+ formation can be observed (Fig. 3b). Because of NH_4^+ dynamics, another proton viz, H_3 becomes closer to O_2 ion in the framework. Consequently, at 490 step O_2–H_3 bond is formed leaving NH_3 back as free molecule. Next, at 720 step this proton (H_3) moves back to NH_3 to form NH_4^+ again. This scenario is repeated with another proton (H_1) when it becomes close to O'_2 it forms O'_2–H_1 bond at 880 step. Thereafter, NH_4^+ is noticed by the 1320 step. By the end of the simulation at 2000 step (Fig. 3g), it can be seen that H_2 and O'_2 form a bond indicating the continuous proton transfer. Another way to follow the dynamics of ammonia protonation–deprotonation during the adsorption process is to plot the N–H bond population viz, N–H_1, N–H_2, N–H_3, and N–H_4 during the dynamics simulations as shown in Fig. 4. This figure shows clearly when NH_4^+ is formed during the dynamics simulation. Also it reflects when and which proton is attached to the framework oxygen ion. In more details, the bond population values for all N–H bonds are relatively high when NH_4^+ is formed. However if a bond population value is minimum for a specific N–H_x bond, it means that this proton H_x is attached to the framework oxygen. Accordingly, Fig. 4 shows that three different protons viz., H_3, H_2, and H1 go to framework oxygen ions while NH_4^+ is observed in the meanwhile. Therefore, the dynamics study reveals that there are three oxygen ions in the framework, around the aluminum ion, involved in the interaction with NH_4^+ ion. Furthermore, there is a continuous and consecutive transfer of the protons between the NH_4^+ and the neighboring lattice oxygen ions around Al. From the simulation, it seems that NH_3 molecule is acting as a bridge facilitating the protons transfer to different oxygen ions. This point of view may interpret the reason for the weak shoulder observed at 3375 cm^{-1} [15]. It should be mentioned here that although the quantum molecular dynamics simulation was carried out for short period 0.2 ps, it was sufficient to monitor the protonation–deprotonation event of NH_3 on the Brønsted acid site in the main channel of H-MOR.

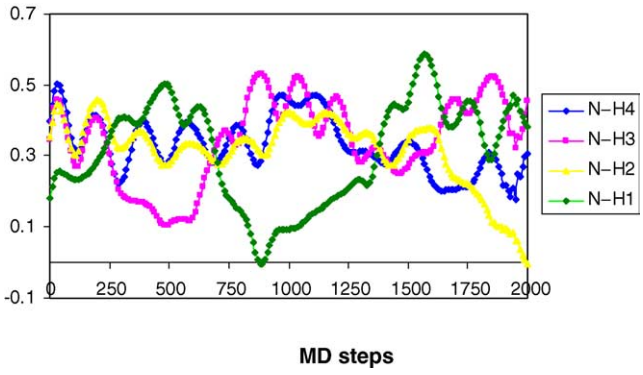

Fig. 4. N—H_x bond population analysis during the molecular dynamics simulation of NH_3 adsorption.

4. Conclusions

The relative strength of the four Brønsted acid sites in H-MOR are investigated using DF method. It has been found that Brønsted acid sites at (T_1, T_2, and T_4) in the main channel are stronger than Brønsted acid site in the side pocket at T_3 site. Moreover, molecular dynamics simulation of NH_3 adsorption on Brønsted acid site in the main channel could monitor the protonation–deprotonation of ammonia resulting from the continuous protons transfer in between ammonium ion and oxygen ions in the framework.

Acknowledgements

M. Elanany thanks the Japanese government and the Belgian interuniversity program (PAI/IUAP5/01) for the financial support.

References

[1] M. Maache, A. Janin, J.C. Lavalley, E. Benazzi, Zeolites 15 (1995) 507.
[2] H. Knözinger, S. Huber, J. Chem. Soc., Faraday Trans. 94 (1998) 2047.
[3] C. Lee, D.J. Parrillo, R.J. Gorte, W.E. Farneth, J. Am. Chem. Soc. 18 (1996) 3262.
[4] M. Bevilacqua, G. Busca, Catal. Commun. 3 (2002) 497.
[5] N. Katada, H. Igi, J. Kim, M. Niwa, J. Phys. Chem. B 101 (1997) 5969.
[6] T. Miyamoto, N. Katada, J. Kim, M. Niwa, J. Phys. Chem. B 102 (1998) 6738.
[7] N. Katada, Y. Kageyama, M. Niwa, J. Phys. Chem. B 104 (2000) 7561.
[8] F. Yin, A.L. Blumenfeld, V. Gruver, J.J. Fripiat, J. Phys. Chem. B 101 (1997) 1824.
[9] M. Elanany, M. Koyama, M. Kubo, P. Selvam, A. Miyamoto, Micropor. Mesopor. Mater. 71 (2004) 51.
[10] M. Elanany, M. Koyama, M. Kubo, E. Brocklawik, A. Miyamoto, Appl. Surf. Sci. 246 (2005) 96.
[11] A.A. Lamberov, A.M. Kuznetov, M.S. Shapnik, A.N. Masliy, S.V. Borisevich, R.G. Romanova, S.R. Egorova, J. Mol. Catal. A 158 (2000) 481.
[12] J. Sauer, P. Ugliengo, E. Garrone, V. Saunders, Chem. Rev. 94 (1994) 2095.
[13] E.H. Teunissen, R.A. van Santen, A.P.J. Jansen, F.B. van Duijneveldt, J. Phys. Chem. 97 (1993) 203.
[14] S.P. Yuan, J.G. Wang, Y.W. Li, H. Jiao, J. Mol. Struct. (Theochem.) 674 (2004) 267.
[15] A. Zecchina, L. Marchese, S. Bordiga, C. Paze, E. Gianotti, J. Phys. Chem. B 101 (1997) 10128.
[16] A. Dyer, A.P. Singh, Zeolites 8 (1988) 242.
[17] Mobil Oil Corporation, US patent 4419220.
[18] J.N. Israelachvili, Intermolecular and Surface Forces", 2nd ed., Academic Press, London, 1992, p. 31.
[19] L. Benco, Th. Demuth, J. Hafner, F. Hutschka, Chem. Phys. Lett. 324 (2000) 373.
[20] Th. Demuth, L. Benco, J. Hafner, H. Toulhoat, Inter. J. Quant. Chem. 84 (2001) 110.
[21] I. Stich, J.D. Gale, K. Terakura, M.C. Payne, J. Am. Chem. Soc. 121 (1999) 3292.
[22] F. Haase, J. Sauer, Micropor. Mesopor. Mater. 35 (2000) 379.
[23] M. Elanany, K. Sasata, T. Yokosuka, S. Takami, M. Kubo, A. Miyamoto, Stud. Surf. Sci. Catal. 142 (2002) 1867.
[24] R.J. Gorte, Catal. Today 28 (1996) 405.
[25] T. Bucko, J. Hafner, L. Benco, J. Chem. Phys. 120 (2004) 10263.
[26] M. Elanany, P. Selvam, T. Yokosuka, S. Takami, M. Kubo, A. Imamura, A. Miyamoto, J. Phys. Chem. B 107 (2003) 1518.
[27] W.M. Meier, D.H. Oslon, Ch. Baerlocher, Atlas of Zeolite Structure Types, 4th (rev.) ed., Butterworths, London, 1996.
[28] A. Alberti, P. Davoli, G. Vezzalini, Z. Kristallogr. 175 (1986) 249.
[29] M. Brändle, J. Sauer, J. Am. Chem. Soc. 120 (1998) 1556.
[30] T. Demuth, J. Hafner, L. Benco, H. Toulhoat, J. Phys. Chem. B. 104 (2000) 4593.
[31] Software from Accelrys Inc., www.accelrys.com.
[32] B. Delley, D.E. Ellis, A.J. Freeman, E.J. Baerends, D. Post, Phys. Rev. B 37 (1983) 2132.
[33] B. Delley, J. Chem. Phys. 92 (1990) 508.
[34] S.H. Vosko, L. Wilk, M. Nusair, Can. J. Phys. 58 (1980) 1200.
[35] J.P. Perdew, J.A. Chevary, S.H. Vosko, K.A. Jackson, M.R. Pederson, D.J. Singh, C. Fiolhais, Phys. Rev. B 46 (1992) 6671.
[36] T. Yokosuka, H. Kurokawa, S. Takami, M. Kubo, A. Miyamoto, A. Imamura, Jpn. J. Appl. Phys. 41 (2002) 2410.
[37] K. Sasata, T. Yokosuka, H. Kurokawa, S. Takami, M. Kubo, A. Imamura, T. Shinmura, M. Kanoh, P. Selvam, A. Miyamoto, Jpn. J. Appl. Phys. 42 (2003) 1859.
[38] M. Kubo, M. Ando, S. Sakahara, C. Jung, K. Seki, T. Kusagaya, A. Endou, S. Takami, A. Imamura, A. Miyamoto, A. Appl. Surf. Sci. 223 (2004) 188.
[39] A. Martucci, G. Cruciani, A. Alberti, C. Ritter, P. Ciambelli, M. Rapacciuolo, Micropor. Mesopor. Mater. 35/36 (2000) 405.